iScience

CellPress
OPEN ACCESS

Article

IL-27 mediates immune response of pneumococcal vaccine SPY1 through Th17 and memory CD4^{+}T cells

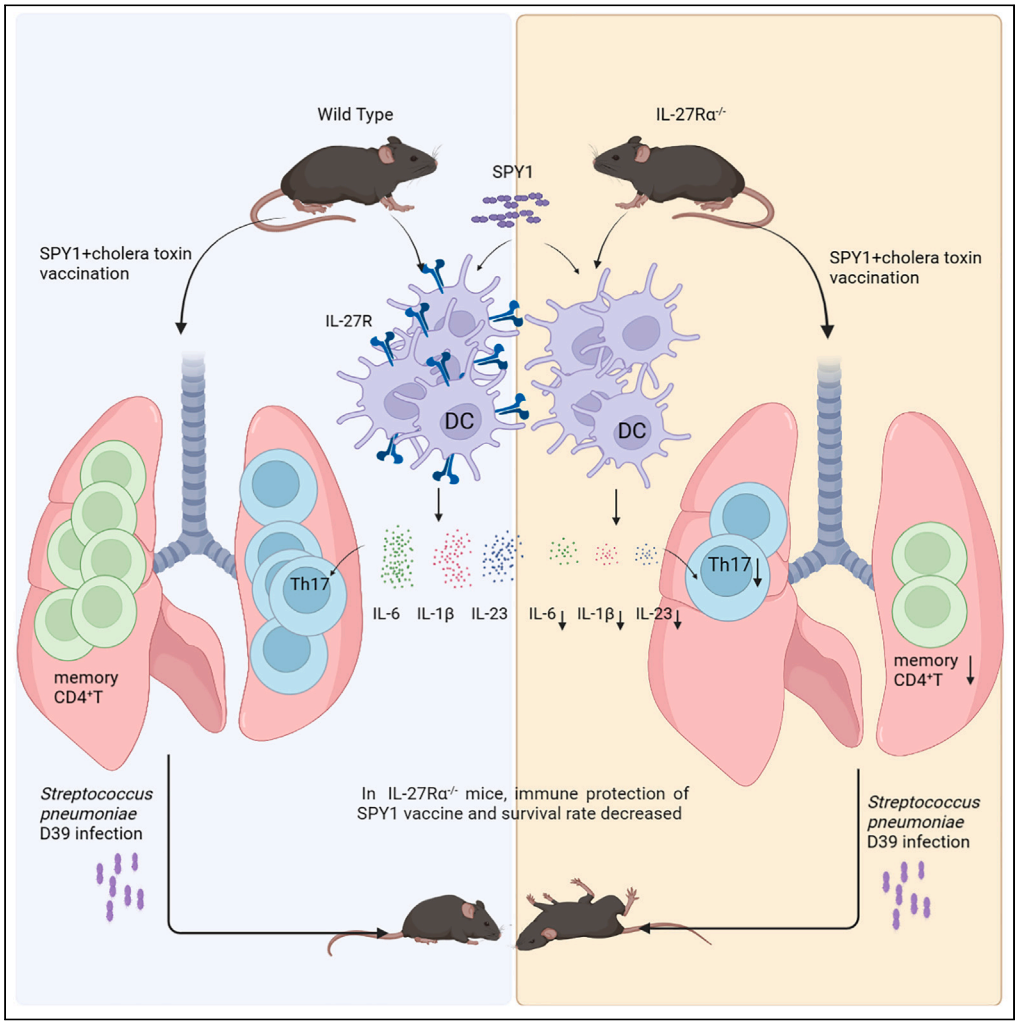

Yanyu Zhang, Song Gao, Shifei Yao, ..., Xuemei Zhang, Hong Wang, Wenchun Xu

xuwen@cqmu.edu.cn

Highlights

IL-27 plays a protective role in pneumococcal vaccine SPY1

IL-27 promotes Th17 cell immune response in SPY1 vaccination

IL-27 promotes the production of memory CD4^{+}T cells in SPY1 vaccination

The immune protection of SPY1 vaccine is independent of glycolysis

Zhang et al., iScience 26, 107464
August 18, 2023
https://doi.org/10.1016/j.isci.2023.107464

iScience

CellPress
OPEN ACCESS

Article

IL-27 mediates immune response of pneumococcal vaccine SPY1 through Th17 and memory CD4$^+$T cells

Yanyu Zhang,[1,3] Song Gao,[2,3] Shifei Yao,[1] Danlin Weng,[1] Yan Wang,[1] Qi Huang,[1] Xuemei Zhang,[1] Hong Wang,[1] and Wenchun Xu[1,4,*]

SUMMARY

Vaccination is an effective means of preventing pneumococcal disease and SPY1 is a live attenuated pneumococcal vaccine we obtained earlier. We found IL-27 and its specific receptor (WSX-1) were increased in SPY1 vaccinated mice. Bacterial clearance and survival rates were decreased in SPY1 vaccinated IL-27Rα$^{-/-}$ mice. The vaccine-induced Th17 cell response and IgA secretion were also suppressed in IL-27Rα$^{-/-}$ mice. STAT3 and NF-κB signaling and expression of the Th17 cell polarization-related cytokines were also decreased in IL-27Rα$^{-/-}$ bone-marrow-derived dendritic cells(BMDC) stimulated with inactivated SPY1. The numbers of memory CD4$^+$T cells were also decreased in SPY1 vaccinated IL-27Rα$^{-/-}$ mice. These results suggested that IL-27 plays a protective role in SPY1 vaccine by promoting Th17 polarization through STAT3 and NF-κB signaling pathways and memory CD4$^+$T cells production in the SPY1 vaccine. In addition, we found that the immune protection of SPY1 vaccine was independent of aerobic glycolysis.

INTRODUCTION

Streptococcus pneumoniae is an opportunistic pathogen that colonizes the human oral and nasopharyngeal cavities and is the primary cause of pneumonia in the elderly and children under 5 years of age.[1,2] Vaccination is an effective means to prevent pneumococcal disease.[3] However, pneumococcal polysaccharide and conjugate vaccines have deficiencies such as limited serotype coverage, high cost, and vaccine serotype substitution. Therefore, new vaccine candidates are required to overcome these shortcomings.[4,5] Whole-cell pneumococcal vaccines are considered as ideal candidates because of their strong antigenicity and comprehensive serotype coverage.[6] Our laboratory had previously developed a live attenuated vaccine of *S. pneumoniae* (SPY1) that had very low toxicity, reliable genetic stability, high safety, and good protective effect against *S. pneumoniae* infection in a mouse model.[7] Elucidation of the protective mechanism of the vaccine is important for the research and development of this new pneumococcal vaccine.

In previous studies, we reported that SPY1 immunization can enhance humoral and Th2, Th17, and Treg cell immune responses in mice. The Th2 immune response participates in the protective effect of SPY1 on the survival of mice infected with *S. pneumoniae* and Th17 cells and associated inflammatory cell responses are involved in the clearance of colonizing bacteria.[8] SPY1 promoted the production of TGF-β1 and up-regulated SPY1-specific CD4$^+$CD25$^+$Foxp3$^+$Treg cells via the Smad2/3 pathway to enhance immune protection.[9] In addition, SPY1 can activate dendritic cells (DC) via mitogen-activated MAPK and NF-κB signaling pathways and drive the Th17 response. SPY1 effectively stimulated DCs to express IL-1β, IL-23, IL-10, and IL-27.[10] IL-1β and IL-23 are essential for Th17 cell differentiation.[11–13] IL-10 is involved in the induction of CD4$^+$CD25^{hi}Foxp3^{hi}Treg cells that play an important role in maintaining immune homeostasis and can limit excessive inflammatory responses caused by infection.[14–18] However, it is unclear whether the significant increase in IL-27 participates in the protective effect of the SPY1 vaccine immunization.

IL-27 is a multipotent cytokine heterodimer composed of IL-27 p28 and EBI3 subunits and EBI3 is also an IL-35 subunit. IL-27 can directly activate target cells through a high affinity IL-27 receptor (IL-27R), that includes IL-27Rα (WSX-1) and glycoprotein 130 (gp130).[19] IL-27 has anti-inflammatory and pro-inflammatory effects via targeting Th1, Th2, Th17, and Treg and plays an important role in autoimmune disease, tumor growth,

[1]Key Laboratory of Laboratory Medical Diagnostics Designated by the Ministry of Education, School of Laboratory Medicine, Chongqing Medical University, Chongqing, China

[2]Department of Laboratory Medicine, Affiliated Hospital of Zunyi Medical University, School of Laboratory Medicine, Zunyi Medical University, Zunyi, Guizhou, China

[3]These authors contributed equally

[4]Lead contact

*Correspondence: xuwen@cqmu.edu.cn

https://doi.org/10.1016/j.isci.2023.107464

and infections of the central nervous system, lungs, skin, and gastrointestinal tract.[20–23] For example, exogenous IL-27 enhanced early host innate immunity and accelerated bacterial clearance in a *Staphylococcus aureus* bone infection model.[24] IL-27 can also inhibit clearance of *Mycobacterium tuberculosis*.[25]

IL-27 is also linked to memory T cell formation and induces IL-10 production by tumor antigen-specific $CD8^+$T cells that contribute to T cell memory.[26] In contrast, IL-27 signaling inhibits the formation of memory $CD4^+$T cells in mice in secondary malaria infections.[27]

IL-27 plays a central role in T cell immune responses to subunit vaccines. The antigenic subunit of these vaccines can only produce effective neutralizing antibodies, while the induction of a large number of antigen-specific T cells requires corresponding adjuvant.[28] IL-27 signaling also affects the production of high affinity antigen specific $CD4^+$ and $CD8^+$T cells in combined TLR/CD40 vaccination.[29] IL-27 can also promote the clonal proliferation of subunit vaccine-induced specific T cells by affecting the tricarboxylic acid cycle in mitochondrial metabolism rather than aerobic glycolysis.[30] Eomesodermin (Eomes) is an important transcription factor in T cell polarization, that can regulate CD122 expression that supports the proliferation and survival of T cells via IL-2/15 signaling.[31,32] IL-27 can amplify Eomes expression via STAT3.[33,34] In combined TLR/CD40 vaccination, IL-27Rα deficiency resulted in decreased expression of Eomes and CD122, as well as memory T cell expansion and survival.[29] The production of IL-27 p28 is directly related to the cellular memory of downstream $CD8^+$T cells and protection in the immune-response induced by subunit vaccines.[35] These studies suggested that IL-27 plays an important protective role in vaccines. However, in neonatal BCG (Bacillus Calmette–Guérin) immunization, increased IL-27 inhibited uptake of BCG by DCs, thus inhibiting their immunological protection.[36] Therefore, the role of IL-27 in vaccine immunity is pleiotropic.

The role and mechanism of IL-27 in *S. pneumoniae* whole-cell vaccine SPY1 are still unclear. In this study, we investigated the effect of IL-27 on SPY1 vaccine and its mechanism.

RESULTS

IL-27 expression increases in mice immunized with SPY1 vaccine

We examined the role for IL-27 in *S. pneumoniae* vaccine SPY1 following immunization of C57BL/6 mice using SPY1. The mice were intranasally immunized according to the vaccination procedure described in Figure 1A. On the 28th day, we examined mouse lung tissues. The mRNA expression levels of the IL-27 subunits *P28* and *Ebi3* and a specific IL-27 receptor subunit *Wsx-1* were all elevated in the vaccine groups compared to the PBS controls. EBI3 is also an IL-35 subunit when combined with p35 so we also measured *P35* expression. We found no significant differences between the vaccinated and control tissues so that IL-35 did not contribute to the increased EBI3 levels (Figure 1B). IL-27 protein levels in the lung tissue and nasal lavage fluid from the vaccinated groups were also significantly greater than controls. IL-27 protein levels were also increased in serum samples of vaccinated mice but were not statistically different from the control group (Figure 1C). These data indicated that IL-27 and its specific receptor subunit WSX-1 were up-regulated in mice vaccinated with SPY1 implicating IL-27 as an immune regulator for this vaccine.

IL-27Rα deficiency inhibits the immune protective effect of SPY1 vaccine

To determine the effect of IL-27 on SPY1 vaccine, we inoculated wild-type (WT) mice and IL-27R$\alpha^{-/-}$ (KO) mice with SPY1 vaccine and established a colonizing infection model using *S. pneumoniae* strain 19F (Figure 2A). The bacterial loads in nasal lavage fluids from the WT mice in the vaccine group were significantly less than controls. In contrast, bacterial loads between vaccinated and control IL-27R$\alpha^{-/-}$ mice displayed no significant differences (Figure 2B). WT and IL-27R$\alpha^{-/-}$ mice were then challenged with a lethal dose of *S. pneumoniae* D39 one week after the last SPY1 immunization. Survival for the IL-27R$\alpha^{-/-}$ mice was significantly less than for the WT mice (Figure 2C). Since macrophages and neutrophils are key effector cells in clearing *S. pneumoniae*, we observed the recruitment of macrophages and neutrophils in mice lung tissues. Three days following 19F challenge, H&E staining of lung tissues demonstrated that inflammatory cell numbers for the WT SPY1-immunized mice were elevated compared with controls. In contrast, IL-27R$\alpha^{-/-}$ mice displayed no differences from their controls. In the SPY1 immunization group, the levels of neutrophils and macrophages in the lungs of KO mice were significantly lower than those of WT mice (Figures 2D–2G). These results suggested that IL-27Rα deficiency inhibits the immune protective effect of SPY1 vaccine.

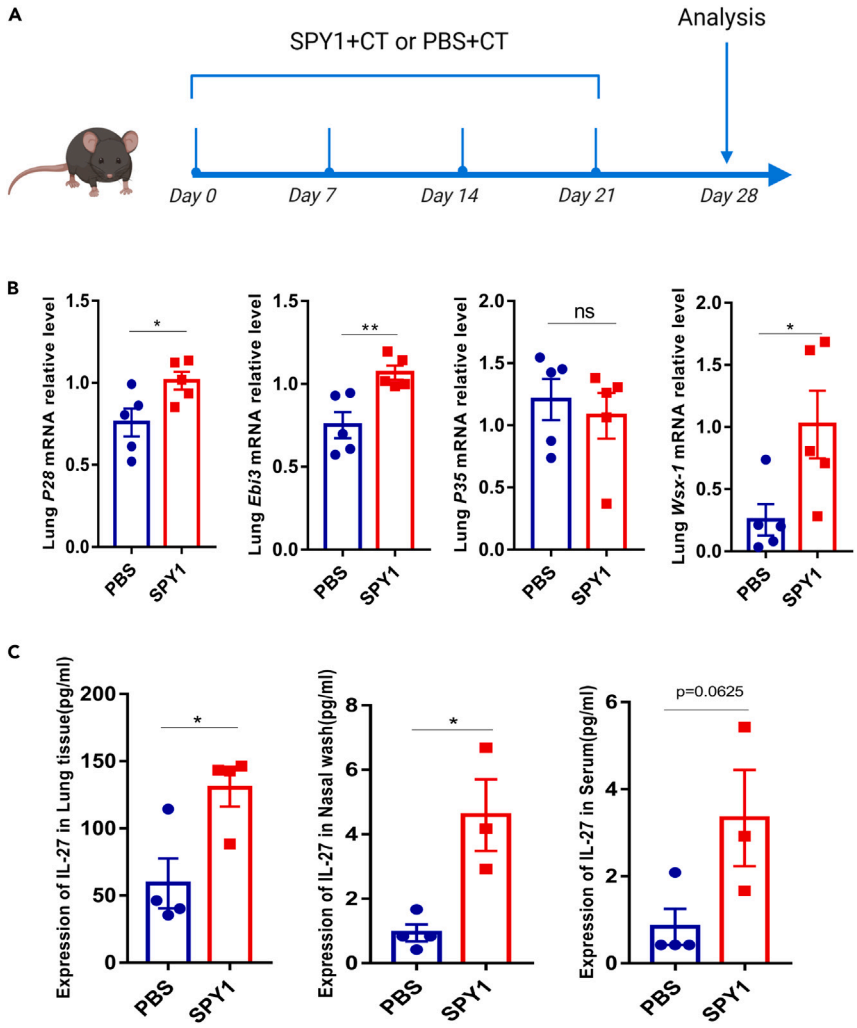

Figure 1. IL-27 expression is increased by SPY1 immunization

(A) Mice were intranasally immunized with SPY1 plus CT or PBS plus CT weekly for 1 month and specimens were collected for analysis on day 28.

(B) mRNA expression levels of the IL-27 subunits p28, EBI3, the IL-35 subunits p35, and the IL-27 receptor subunit WSX-1 (n = 5). T-test. Mean ± SEM.*p < 0.05, **p < 0.01.

(C) Protein levels of IL-27 in lung tissues, nasal washes and serum of mice determined by ELISA (n = 3–4). T-test. Mean ± SEM. *p < 0.05. CT, cholera toxin adjuvant.

IL-27Rα deficiency inhibits the Th17 cell immune response in SPY1 vaccination

Our laboratory had previously reported that SPY1 immune protection is primarily dependent on humoral and Th2, Th17, and Treg cellular immunity.[8] Therefore, we vaccinated WT and IL-27Rα$^{-/-}$ mice with the SPY1 vaccine to explore the mechanism by which IL-27 contributes to the protective effect of SPY1 vaccine. We measured specific antibody production along with cytokine levels. The IgG titers of both WT and IL-27Rα$^{-/-}$ vaccinated mice were significantly higher than those of PBS controls, while there was no significant difference between the WT and KO vaccinated mice. However, SPY1-specific IgA titers of the vaccinated IL-27Rα$^{-/-}$ mice were significantly lower than those of WT mice (Figure 3A). These results suggested that IL-27Rα deficiency does not affect the production of specific IgG but affects the production of specific IgA after SPY1 immunization.

Consistent with these results is another study indicating that vaccine-induced Th17 cells can form tissue-resident cells in the lung to promote local IgA responses.[37] We further discovered that IL-17A levels in both lung and spleen WT tissues of the SPY1 vaccine group were significantly higher than PBS controls.

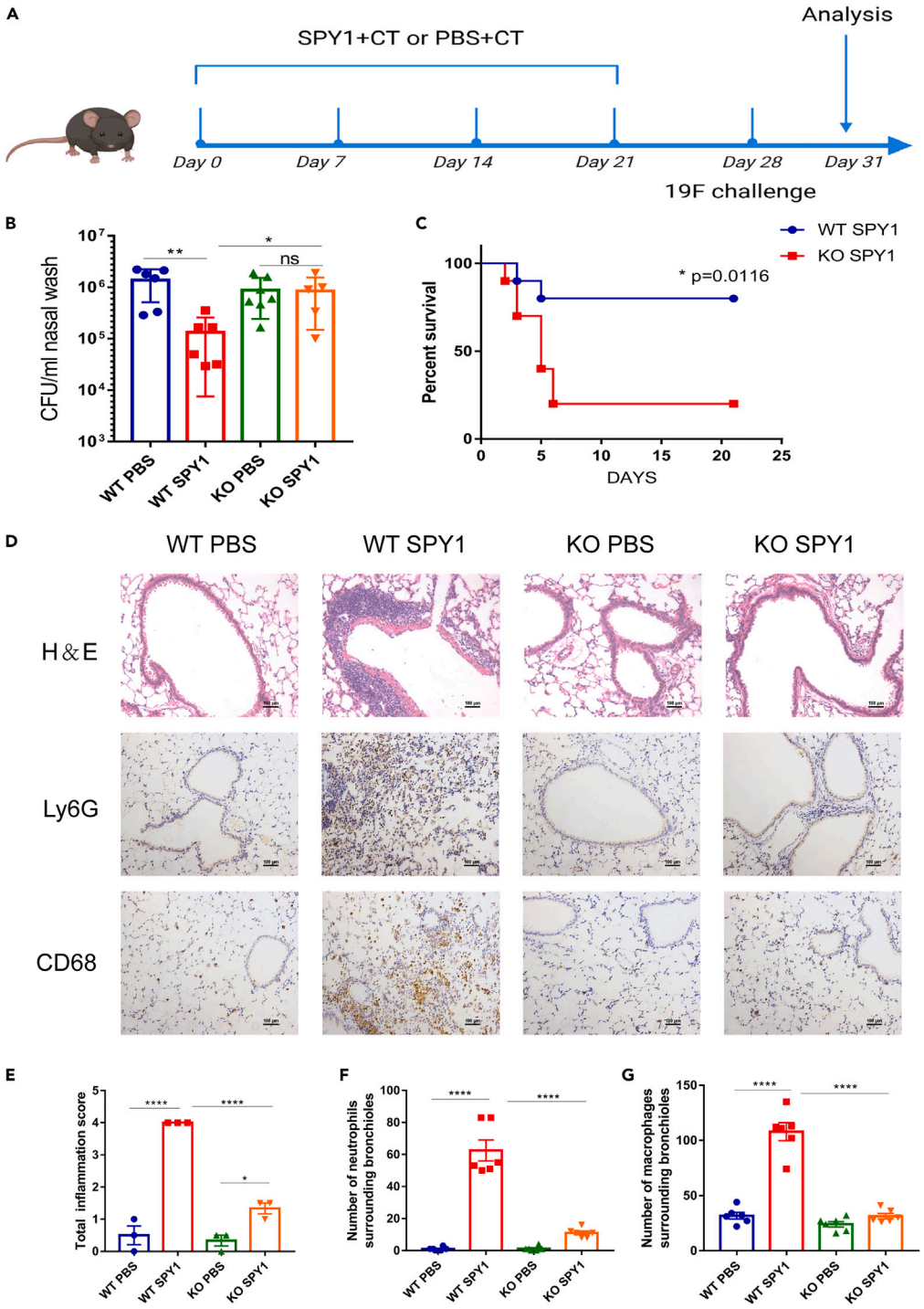

Figure 2. IL-27Rα deficiency halts the protective effect of the SPY1 vaccine

(A) Mice were intranasally immunized with SPY1 plus CT or PBS plus CT weekly for 1 month. On day 28, mice were intranasally challenged with *S. pneumoniae* strain 19F and specimens were collected for analysis on day 31.

(B). Bacterial colonization in nasal lavage fluid of each group after 19F challenge (n = 5–7). One-way ANOVA. Mean ± SEM.*$p < 0.05$, **$p < 0.01$.

(C) One week following the last immunization, mice were challenged intranasally with *S. pneumoniae* strain D39 (5×10^7 CFU). The survival rates were observed for 21 days post challenge (n = 10). Log rank test.*$p < 0.05$.

Figure 2. *Continued*

(D) H&E and peroxidase immune staining for Ly6G (neutrophil marker) and CD68 (macrophage marker) in the indicated groups 3 days after 19F challenge. Representative slides are shown for each group (200 ×; scale bars = 100 μm).
(E) Total inflammation score. One-way ANOVA. Mean ± SEM.*p < 0.05, **p < 0.01, ***p < 0.001, ****p < 0.0001.
(F) Quantification of neutrophils surrounding bronchioles from (D). One-way ANOVA. Mean ± SEM.*p < 0.05, **p < 0.01, ***p < 0.001, ****p < 0.0001.
(G) Quantification of macrophages surrounding bronchioles from (D). One-way ANOVA. Mean ± SEM. *p < 0.05, **p < 0.01, ***p < 0.001, ****p < 0.0001.

In IL-27Rα$^{-/-}$ mice, IL-17A in the lungs of the SPY1 group was also significantly higher than controls but this was not the case for IL-17A in the spleen. However, IL-17A levels in the lung tissue of vaccinated KO mice were significantly lower than those of WT mice (Figure 3B). IFN-γ and IL-5 protein levels in lung and spleen tissues were not significantly different between our experimental groups (Figures 3C and 3D).

We further detected the distribution of T cell subsets in mouse lung tissues by flow cytometry. The number of Th1 and Th2 cells in the SPY1 group increased compared with the control group (no statistical difference), and there was no difference in the proportion of Treg cells among different groups, but the number of Treg cells in IL-27Rα$^{-/-}$ immunized mice was significantly less than that in WT immunized mice. The immunized KO mice also displayed a lower percentage and number of Th17 cells than WT mice (Figures 3E–3I). The above results suggested that IL-27Rα deficiency inhibited Th17 and Treg cell responses and IgA response in SPY1 vaccine.

SPY1 vaccine promotes the production of Th17 differentiation related factors in DCs by IL-27

Th17 cells can recruit macrophages and neutrophils that play essential protective role in *S. pneumoniae* infections.[38] Our previous study suggested that SPY1-activated DC could promote Th17 differentiation[10] and IL-1β, IL-6, TGF-β, and IL-23 are key cytokines required for Th17 differentiation.[39] To investigate whether IL-27 acts on DC cells to affect Th17 differentiation in SPY1 vaccine immunization, we treated IL-27Rα$^{-/-}$ and WT BMDC with inactivated SPY1. We found no significant differences in TGF-β protein levels among the different groups. In BMDC derived from both WT and KO mice, protein and mRNA levels of IL-6 and IL-1β and the mRNA expression of IL-23A in SPY1 treatment groups were significantly higher than the PBS control groups. These results suggested that SPY1 can promote the secretion of IL-6, IL-1β, and IL-23A in DC cells. Additionally, IL-6, IL-1β, and IL-23A levels in WT BMDC treated with SPY1 were significantly higher than those in KO BMDC (Figures 4A and 4B). At the same time, we treated SPY1-stimulated BMDC with recombinant IL-27 and found that IL-27 could enhance the stimulation of SPY1 on BMDC and further promote the production of IL-6 and IL-1β by BMDC (Figure S1). Collectively, these results indicated that IL-27 can promote the production of IL-6, IL-1β, and IL-23, the key cytokines of Th17 differentiation in DC cells stimulated by SPY1.

To further explore the mechanism of IL-27 in DCs, BMDC from IL-27Rα KO mice and WT mice were treated with inactivated SPY1. STAT3 and NF-κB phosphorylation were significantly higher in WT and IL-27Rα KO BMDC compared with their respective controls. However, phosphorylation levels of STAT3 and NF-κB of the KO group were significantly lower than those of the WT group (Figures 4C and 4D). This suggested that IL-27 is involved in the activation of SPY1 on DC cells through STAT3 and NF-κB signaling pathways.

IL-27Rα deficiency suppresses STAT3 signaling in CD4$^+$T cells and reduces production of memory CD4$^+$T cells in SPY1 vaccine

The long-term protective effect of vaccines is related to immune memory. We, therefore, examined whether IL-27 affects cellular memory following SPY1 immunization by quantifying CD4$^+$ memory cell numbers in lung tissues in WT and KO mice two weeks following vaccination. The proportions and numbers of CD4$^+$ central memory T cells (CD4$^+$CD44$^+$CD62L$^+$) in WT mice were significantly higher than those in KO mice but levels of CD4$^+$ effector memory T cells (CD4$^+$CD44$^+$CD62L$^-$CD127$^+$) did not differ (Figures 5A and 5B). This suggested that IL-27Rα deficiency inhibits the generation of CD4$^+$T memory cells during immunization with SPY1 vaccine.

STAT3 plays an important role in the formation of memory T cells[40] so we examined STAT3 activation of CD4$^+$T cells in lung tissues of WT and KO mice immunized with SPY1. We found that STAT3 activation in CD4$^+$T cells of WT mice was significantly higher than that of the KO mice (Figure 5C). Together, these

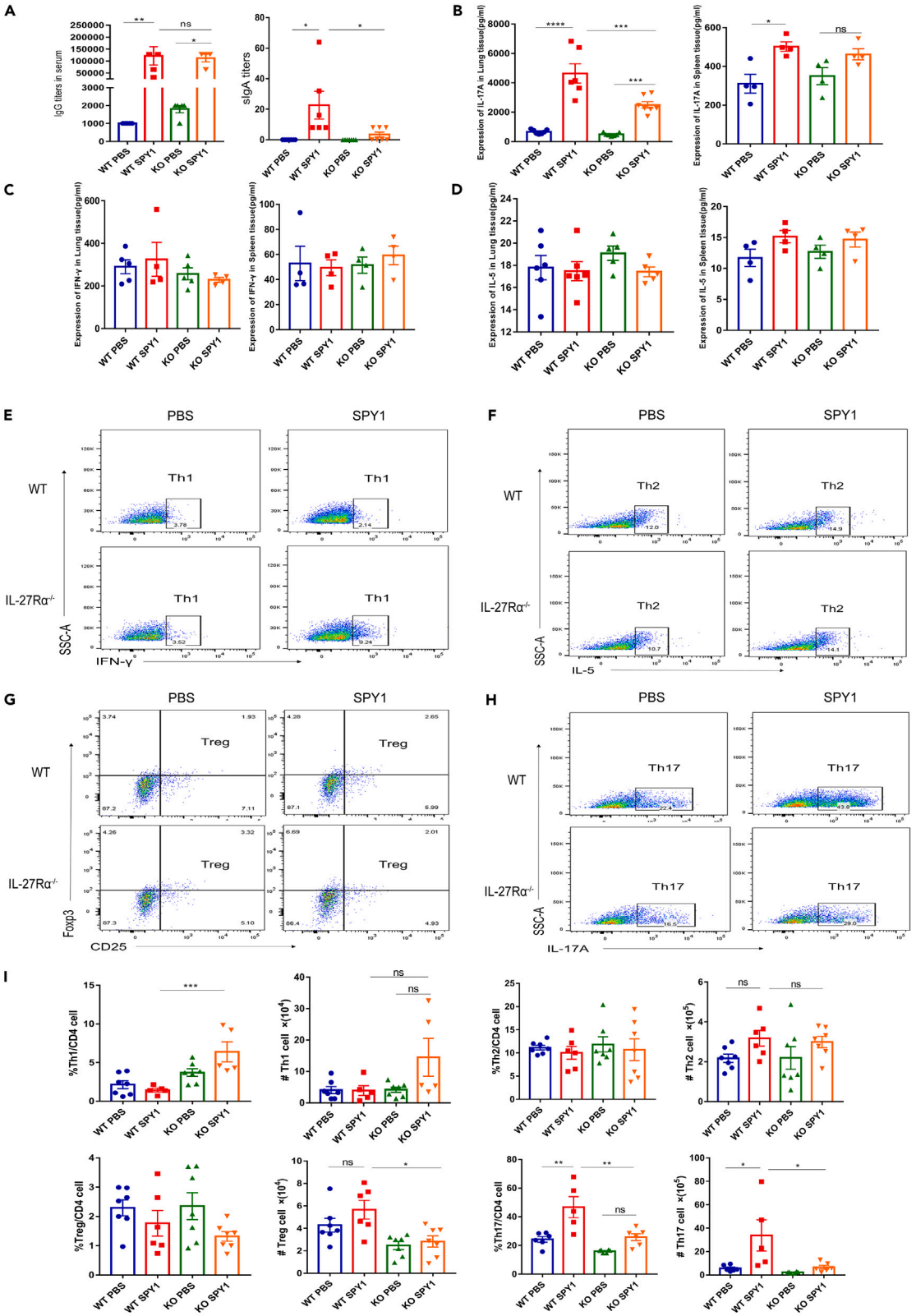
A
IgG titers in serum
sIgA titers
B
Expression of IL-17A in Lung tissue(pg/ml)
Expression of IL-17A in Spleen tissue(pg/ml)
C
Expression of IFN-γ in Lung tissue(pg/ml)
Expression of IFN-γ in Spleen tissue(pg/ml)
D
Expression of IL-5 in Lung tissue(pg/ml)
Expression of IL-5 in Spleen tissue(pg/ml)
WT PBS
WT SPY1
KO PBS
KO SPY1
E
PBS
SPY1
WT
IL-27Rα-/-
Th1
SSC-A
IFN-γ
F
Th2
IL-5
G
Treg
Foxp3
CD25
H
Th17
IL-17A
I
%Th1/CD4 cell
Th1 cell ×(10⁴)
%Th2/CD4 cell
Th2 cell ×(10⁵)
%Treg/CD4 cell
Treg cell ×(10⁴)
%Th17/CD4 cell
Th17 cell ×(10⁵)

Figure 3. IL-27Rα deficiency inhibits the Th17 cell immune response in SPY1 vaccinated mice

(A) Titers of IgG in serum and sIgA in saliva (n = 5–7). One-way ANOVA. Mean ± SEM.*p < 0.05, **p < 0.01.

(B–D) Protein (ELISA) levels of (B) IL-17A (C) IFN-γ and (D) IL-5 in mice 3 days following 19F challenge in lung and spleen tissues (n = 4–7). One-way ANOVA. Mean ± SEM.*p < 0.05, **p < 0.01, ***p < 0.001, ****p < 0.0001.

(E–H) Representative flow cytometric plots depicting proportions of (E) Th1 (F) Th2 (G) Treg and (H) Th17 cells in the indicated experimental groups.

(I) Proportions and numbers of Th1, Th2, Treg, and Th17 cells in the indicated groups as assessed by flow cytometry (n = 5–7). One-way ANOVA. Mean ± SEM. *p < 0.05, **p < 0.01, ***p < 0.001.

results indicated that IL-27 produced following SPY1 vaccination may promote memory cell formation by acting on STAT3 signaling in $CD4^+$T cells.

The immune protection of SPY1 vaccine is independent of glycolysis

Cellular metabolism is closely related to immune function.[41] We, therefore, treated WT SPY1-immunized mice with the glycolytic inhibitor 2-DG to establish a model of *S. pneumoniae* colonization. We found no significant differences in IgA titers in saliva and IgG titers in blood between 2-DG-treated and control mice (Figure 6A). Following 19F challenge, staining of lung tissues indicated that 2-DG treatment did not inhibit neutrophils and macrophages recruitment after SPY1 immunization (Figure 6B) and IL-17A levels in lung tissues did not differ between experimental and control samples (Figure 6C). In addition, the proportions and numbers of Th17 cells in lung tissues were not altered (Figures 6D and 6E). These results indicated that both humoral and Th17 cellular immunity were not dependent on glycolysis to mount a protective effect following SPY1 immunization.

DISCUSSION

Whole-cell *S. pneumoniae* vaccines do not possess the disadvantages of high cost and serotype substitution seen in conjugate vaccines. They also retain the pathogen-related molecular patterns recognized by host antigen-presenting cells and can produce stronger and broader protective effects and the production process is greatly simplified. In particular, pneumococcal whole-cell vaccines may be a better option for developing countries.[4–6] Moreover, it is also essential that the immune protection mechanism for these vaccines be identified. The underlying protective mechanism for the whole-cell *S. pneumoniae* vaccines SPY1 had not been fully elucidated. In this study, we found that expression of IL-27 and its receptor IL-27Rα increased in WT mice following SPY1 immunization, and the protection against *S. pneumoniae* infection was decreased in IL-27R$\alpha^{-/-}$ mice immunized with SPY1. Moreover, IL-27Rα deficiency inhibited Th17 and memory $CD4^+$T cells production in SPY1 vaccinated mice, inhibited STAT3 and NF-κB activation, and inhibited production of Th17 polarity-related factors including IL-6, IL-1β, and IL-23A in DCs stimulated by SPY1. These results suggested that IL-27 is involved in the immune protection of SPY1 vaccine by affecting Th17 cells and memory $CD4^+$T cells.

Previous studies have demonstrated that the mechanism of IL-27 action can vary with vaccine type. The development and functions of $CD8^+$T cells induced by adenovirus type 5 (Ad5) vaccine vectors were inhibited by IL-27-induced inhibitory IL-10^+CD4^+T cells.[42] The BCG clearance, antigen presentation and T cell polarization of antigen-presenting cells (macrophages and DC) were inhibited by IL-27 signaling in BCG immunization.[36,43] In contrast, IL-27 can enhance antigen presentation and T cell polarization of mononuclear-derived DC.[44] Meanwhile, IL-27 was required for the formation of high affinity antigen-specific T cells in combined TLR/CD40 vaccination.[29] The combination of recombinant IL-27 as a low-dose potent adjuvant with LyUV or γ-irradiated cancer cells enhances the protection of prophylactic cancer vaccines in a murine melanoma model, although this protective effect was only seen in the initial tumor challenge but not in tumor rechallenge.[45] Our previous study demonstrated that IL-27 expression was significantly increased in DC cells treated with inactivated SPY1.[10] Here, we found that the expression of IL-27 and its specific receptor increased following SPY1 vaccination and IL-27Rα deficiency decreased *S. pneumoniae* clearance and survival following *S. pneumoniae* infection. These results confirmed the protective effect of IL-27 in the whole-cell *S. pneumoniae* vaccine SPY1.

Our previous study found that the SPY1 vaccine promoted the production of IL-17A and IgA in mice and that SPY1 played a protective role via IL-17A and IgA.[8] IgA secretion in the lung is dependent on Th17 cells and the lung IgA response is absent when Th17 cells are depleted. Furthermore, Th17 cells recruit monocytes, macrophages, and neutrophils to mediate cross-mucosal protective immunity in *S. pneumoniae* infections.[37,38,46]

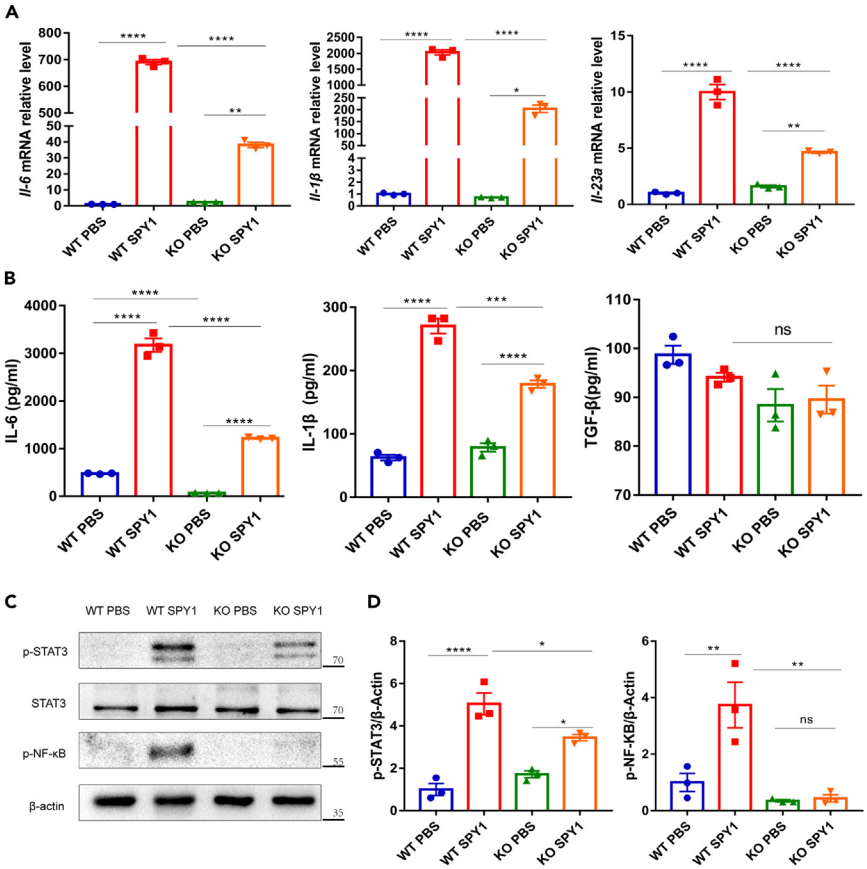

Figure 4. IL-27 promotes the activation of DCs stimulated by SPY1 through STAT3 and NF-κB signaling pathways

(A) BMDC from WT and IL-27Rα KO mice were examined for (A) mRNA levels of IL-6, IL-1β, and IL-23A (n = 3). One-way ANOVA. Mean ± SEM.*p < 0.05, **p < 0.01, ***p < 0.001, ****p < 0.0001.

(B) Protein (ELISA) levels of IL-6, IL-1β, and TGF-β (n = 3). One-way ANOVA. Mean ± SEM.*p < 0.05, **p < 0.01, ***p < 0.001, ****p < 0.0001.

(C) Western blotting to detect phosphorylation states of STAT3 and NF-κB.

(D) Relative densitometric intensity was determined for phosphorylated (p) -STAT3 and NF-κB and then normalized to levels of β-actin (n = 3). One-way ANOVA. Mean ± SEM. *p < 0.05, **p < 0.01, ***p < 0.001, ****p < 0.0001.

IL-27 is involved in the production of IL-17A although IL-27 regulates Th17 cell polarization that is dependent upon stimulating signal and disease model. For instance, in autoimmune encephalomyelitis,[47] chronic inflammation of the central nervous system[48] and viral myocarditis,[49] IL-27 inhibited Th17 cell differentiation by regulating STAT3 and STAT1 signaling. In $CD4^+$T cell, activation of STAT3 signal promotes Th17 cell differentiation while activation of STAT1 signal inhibits Th17 cell differentiation. IL-27 can also promote Th17 cell polarization by acting on antigen-presenting cells to produce IL-6 and IL-1β and aggravate colitis in mice.[50] Our data indicated that IL-27Rα deficiency inhibited the production of Th17 cell polarization-related factors IL-6, IL-1β, and IL-23A in DC cells, thereby inhibiting Th17 cell polarization and lowering the protective effect of the SPY1 vaccine. We also found that IL-27Rα deficiency inhibited STAT3 and NF-κB activation in DC cells following SPY1 treatment. STAT3 has been fully demonstrated to promote DC cell differentiation and function[51] and NF-κB signaling is linked to IL-6 production.[52] In addition, IL-27 can also down-regulate the death receptor ligand FasL and induce expression of anti-apoptotic protein cellular form of Fas-associating protein with death domain(FADD)-like interleukin-1β–converting enzyme(FLICE) inhibitory protein cFLIP via STAT3 signaling to inhibit activation-induced T cell death (AICD). Protection of activated T cells from excessive AICD is crucial for the survival and expansion of T lymphocytes.[53] However, whether IL-27 promotes Th17 cell immune response by inhibiting AICD of $CD4^+$T cells during immunization with SPY1 vaccine needs further research.

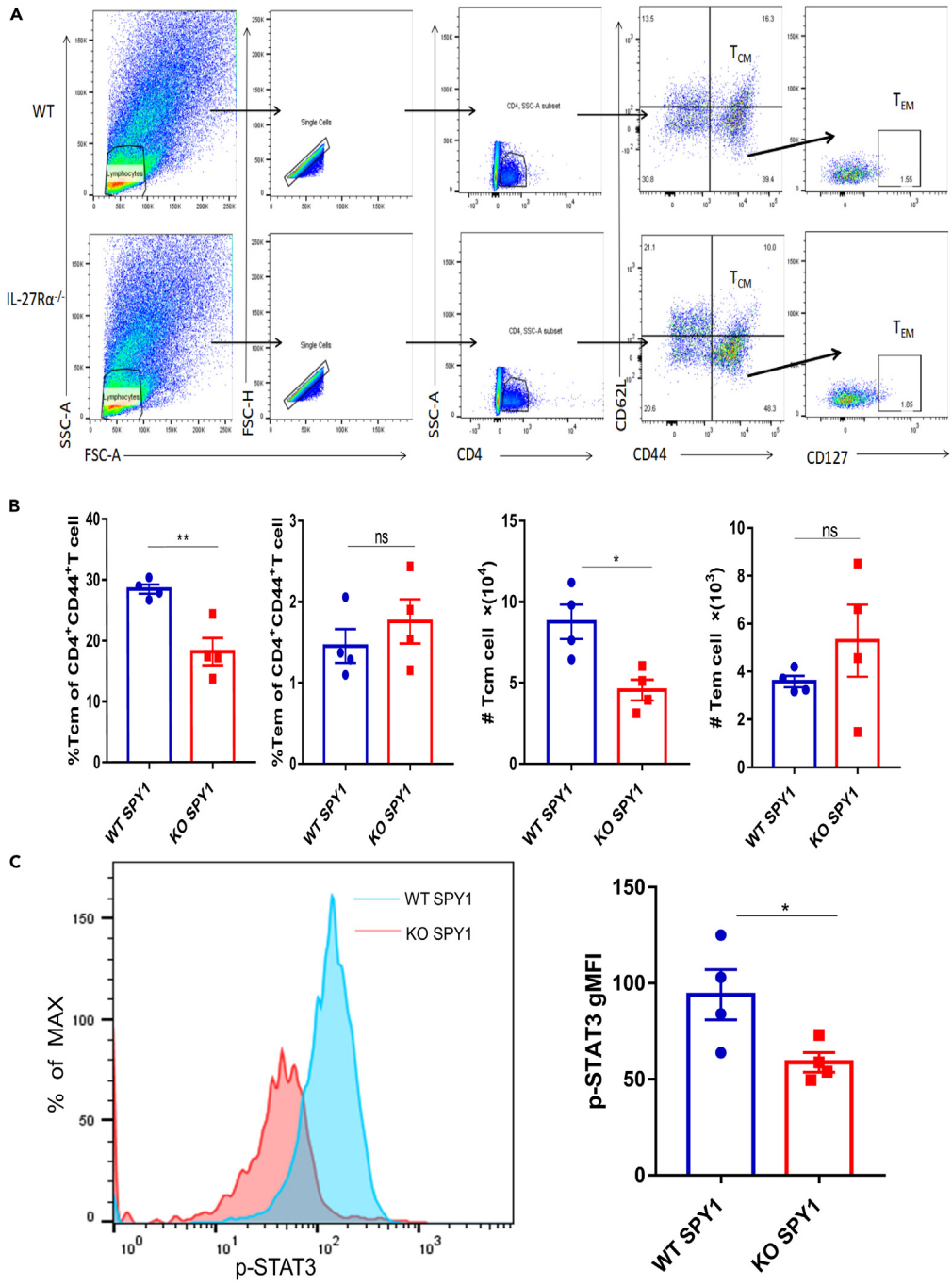

Figure 5. IL-27 inhibits the production of CD4$^+$ memory cells during immunization with SPY1 vaccine

(A) Representative flow cytometric plots showing the proportion of CD4$^+$ memory cells in the indicated experimental groups.

(B) Proportion and numbers of CD4$^+$ memory cells in the indicated groups as assessed by flow cytometry (n = 4). T-test. Mean ± SEM.*p < 0.05, **p < 0.01.

(C) Levels of phosphorylated STAT3 (Y705) in WT SPY1 and KO SPY1 groups assessed by flow cytometry (n = 4). T-test. Mean ± SEM.*p < 0.05.

Immune memory is the key biological process that makes vaccines work and IL-27 is involved in the production of memory cells. For example, in secondary malaria infection, IL-27 signaling inhibits the development of memory CD4$^+$T cells.[27] However, IL-27 is essential for memory cell formation in subunit vaccine adjuvant-

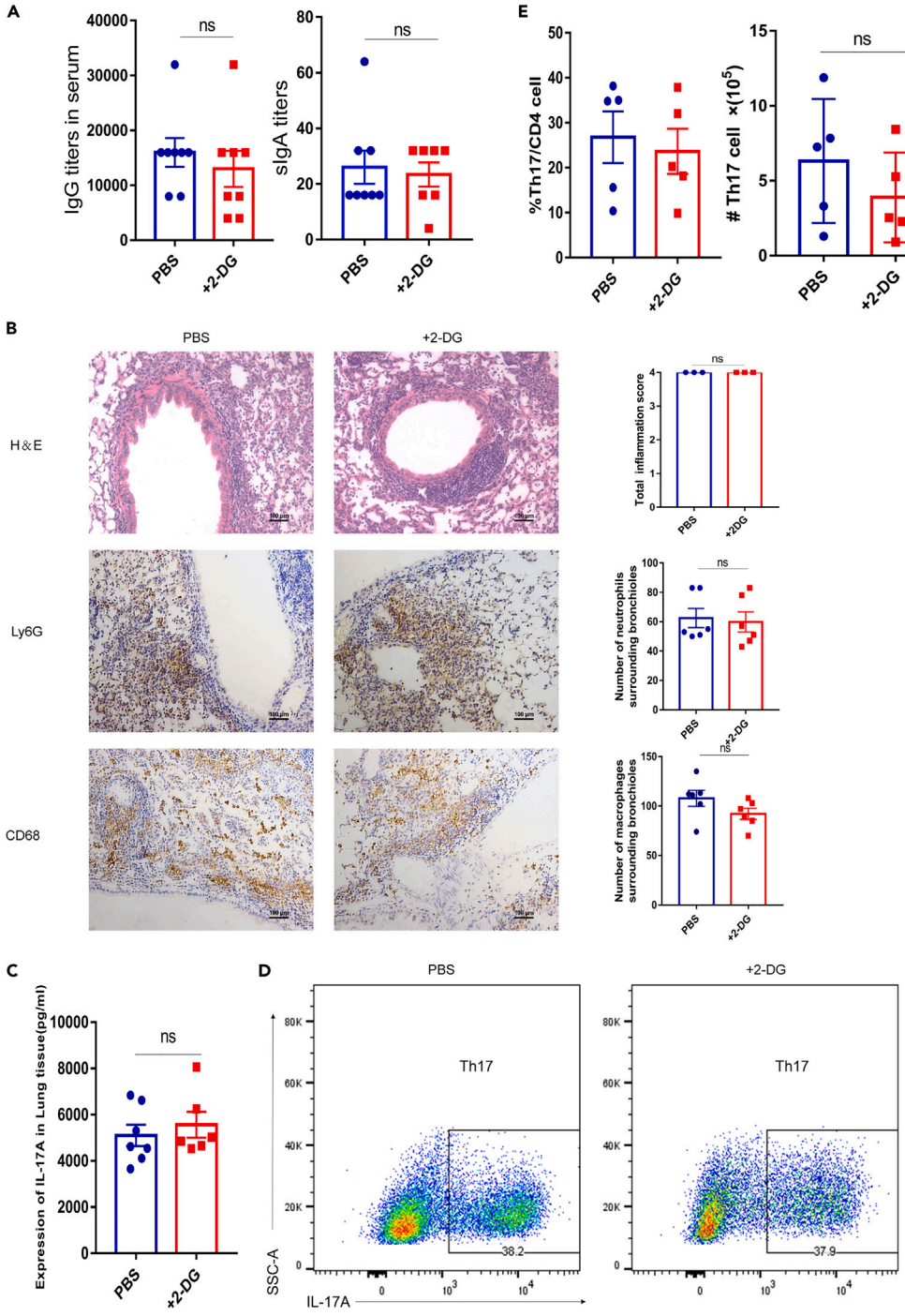

Figure 6. The immune protective effect of SPY1 vaccine is independent of glycolysis

(A) Titers of sIgA in saliva and IgG in serum (n = 7–8). T-test. Mean ± SEM.

(B) H&E staining and peroxidase immune staining in lung tissues for Ly6G and CD68 in WT SPY1 vaccinated mice that were administered either PBS (control) or 2-deoxy-glucose (2-DG) 3 days after 19F challenge. Representative slides are shown for each group (200 ×, scale bars = 100 μm). Total inflammation score and quantification of neutrophils and macrophages surrounding bronchioles (n = 3–6). T-test. Mean ± SEM.

(C) ELISA to quantify IL-17A protein levels in lung tissues (n = 6–7). T-test. Mean ± SEM.

(D) Representative flow cytometric plots depicting proportions of Th17 cells in the indicated groups.

(E) The proportions and numbers of Th17 cells in for the indicated groups determined by flow cytometry (n = 5). T-test. Mean ± SEM.

induced immune responses.[29] It was shown that IL-6/STAT3 signaling is significant for memory cells formation in $CD4^+$T cells.[54] We found that IL-27Rα deficiency suppressed STAT3 signaling in $CD4^+$T cells of lung tissue in mice vaccinated with SPY1. Moreover, the production of memory $CD4^+$T cells decreased after SPY1 immunization in IL-27Rα deficient mice. We, therefore, speculated that the inhibition of memory $CD4^+$T cell formation following IL-27Rα deficiency may be related to the inhibition of IL-6/STAT3 signaling.

Metabolic remodeling is intrinsically related to the differentiation, development, survival, and function of T cells. T cells are associated with different metabolic pathways in their differentiation and activation states. The metabolic pathway in the early stage of T cell activation generally changes from mitochondrial metabolism to aerobic glycolysis. In this metabolic program, rapidly dividing cells mainly convert glucose into lactic acid and produce large amounts of metabolites to maintain activated T cell function.[55,56] IL-27 is also linked to T cell metabolism. In experimental visceral leishmaniasis caused by the human pathogen *Leishmania donovani*, IL-27 signaling limits Th1 cell glycolysis to limit immune damage.[57] However, T cells induced by subunit adjuvant vaccine support clonal expansion only through mitochondrial metabolism. IL-27 also promotes clonal expansion of subunit vaccine-induced T cells by affecting mitochondrial metabolism.[30] In our study, the number and function of Th17 cells in SPY1 vaccine immunity was not affected after inhibition of glycolysis *in vivo* nor was humoral immunity inhibited. These results suggested that T cell metabolism in SPY1 vaccination was not acting via glycolysis. Considering the metabolic pattern of T cells seen following subunit vaccine administration, we hypothesize that T cells metabolized in a mitochondria-dependent manner in SPY1 vaccine immunity and IL-27 may play a vital role in this process.

The results of this study have given a preliminary exploration of the role of IL-27 in immune responsiveness of the *S. pneumoniae* whole-cell vaccine SPY1. This lays a foundation for the research and development of *S. pneumoniae* whole-cell vaccines and to the evaluation of whole-cell vaccine candidates for other pathogenic organisms.

Limitations of the study

In this study, IL-27Rα$^{-/-}$ mice were used. Although it has been proved that the binding of IL-27Rα and gp130 is indispensable in IL-27 signal transduction, IL-27Rα$^{-/-}$ mice can lead to IL-27 signal inhibition. However, in order to further verify the role of IL-27 in SPY1 vaccine, exogenous IL-27 should be supplemented in wild SPY1 immunized mice to observe whether the protective effect is enhanced. Meanwhile, in this study, we have not explored the effect of IL-27 on T cell metabolism in SPY1 vaccine, and it is not clear whether IL-27 promotes T cell cloning and amplification by affecting mitochondrial metabolism.

STAR★METHODS

Detailed methods are provided in the online version of this paper and include the following:

- KEY RESOURCES TABLE
- RESOURCE AVAILABILITY
  - Lead contact
  - Materials availability
  - Data and code availability
- EXPERIMENTAL MODEL AND STUDY PARTICIPANT DETAILS
  - Animal
  - Primary cell
  - Strain
- METHOD DETAILS
  - Flow cytometry analysis
  - RT-PCR analysis
  - Cytokine analysis
  - Antibody titer analysis
  - Western Blot analysis
  - Immunohistochemistry and HE staining
- QUANTIFICATION AND STATISTICAL ANALYSIS

SUPPLEMENTAL INFORMATION

Supplemental information can be found online at https://doi.org/10.1016/j.isci.2023.107464.

ACKNOWLEDGMENTS

This study was supported by a grant from the National Natural Science Foundation of China (Grant No. 81960307 and Grant No. 81671639). We thank the School of Laboratory Medicine, Chongqing Medical University, Chongqing, China; and all the authors involved in this study.

AUTHOR CONTRIBUTIONS

W.X., Y.Z., and S.G. designed the research; Y.Z., S.Y., and Y.W. performed all mouse animal experiments and statistical analysis; Y.Z., Q.H., and D.W. performed cell experiments; X.Z. and H.W. assisted with animal experiments; W.X. and Y.Z. wrote the paper. All authors have read and approved the manuscript.

DECLARATION OF INTERESTS

The authors declare no competing interests.

Received: April 27, 2023
Revised: June 16, 2023
Accepted: July 19, 2023
Published: July 25, 2023

REFERENCES

1. Liu, L., Oza, S., Hogan, D., Perin, J., Rudan, I., Lawn, J.E., Cousens, S., Mathers, C., and Black, R.E. (2015). Global, regional, and national causes of child mortality in 2000-13, with projections to inform post-2015 priorities: an updated systematic analysis. Lancet *385*, 430–440. https://doi.org/10.1016/s0140-6736(14)61698-6.

2. Mitchell, A.M., and Mitchell, T.J. (2010). Streptococcus pneumoniae: virulence factors and variation. Clin. Microbiol. Infect. *16*, 411–418. https://doi.org/10.1111/j.1469-0691.2010.03183.x.

3. Cillóniz, C., Amaro, R., and Torres, A. (2016). Pneumococcal vaccination. Curr. Opin. Infect. Dis. *29*, 187–196. https://doi.org/10.1097/qco.0000000000000246.

4. Flasche, S., Van Hoek, A.J., Sheasby, E., Waight, P., Andrews, N., Sheppard, C., George, R., and Miller, E. (2011). Effect of pneumococcal conjugate vaccination on serotype-specific carriage and invasive disease in England: a cross-sectional study. PLoS Med. *8*, e1001017. https://doi.org/10.1371/journal.pmed.1001017.

5. Balsells, E., Guillot, L., Nair, H., and Kyaw, M.H. (2017). Serotype distribution of Streptococcus pneumoniae causing invasive disease in children in the post-PCV era: A systematic review and meta-analysis. PLoS One *12*, e0177113. https://doi.org/10.1371/journal.pone.0177113.

6. Pichichero, M.E. (2017). Pneumococcal whole-cell and protein-based vaccines: changing the paradigm. Expert Rev. Vaccines *16*, 1181–1190. https://doi.org/10.1080/14760584.2017.1393335.

7. Wu, K., Yao, R., Wang, H., Pang, D., Liu, Y., Xu, H., Zhang, S., Zhang, X., and Yin, Y. (2014). Mucosal and systemic immunization with a novel attenuated pneumococcal vaccine candidate confer serotype independent protection against Streptococcus pneumoniae in mice. Vaccine *32*, 4179–4188. https://doi.org/10.1016/j.vaccine.2014.05.019.

8. Xu, X., Wang, H., Liu, Y., Wang, Y., Zeng, L., Wu, K., Wang, J., Ma, F., Xu, W., Yin, Y., and Zhang, X. (2015). Mucosal immunization with the live attenuated vaccine SPY1 induces humoral and Th2-Th17-regulatory T cell cellular immunity and protects against pneumococcal infection. Infect. Immun. *83*, 90–100. https://doi.org/10.1128/iai.02334-14.

9. Liao, H., Peng, X., Gan, L., Feng, J., Gao, Y., Yang, S., Hu, X., Zhang, L., Yin, Y., Wang, H., and Xu, X. (2018). Protective Regulatory T Cell Immune Response Induced by Intranasal Immunization With the Live-Attenuated Pneumococcal Vaccine SPY1 via the Transforming Growth Factor-β1-Smad2/3 Pathway. Front. Immunol. *9*, 1754. https://doi.org/10.3389/fimmu.2018.01754.

10. Gao, S., Zeng, L., Zhang, X., Wu, Y., Cui, J., Song, Z., Sun, X., Wang, H., Yin, Y., and Xu, W. (2016). Attenuated Streptococcus pneumoniae vaccine candidate SPY1 promotes dendritic cell activation and drives a Th1/Th17 response. Immunol. Lett. *179*, 47–55. https://doi.org/10.1016/j.imlet.2016.08.008.

11. Acosta-Rodriguez, E.V., Napolitani, G., Lanzavecchia, A., and Sallusto, F. (2007). Interleukins 1beta and 6 but not transforming growth factor-beta are essential for the differentiation of interleukin 17-producing human T helper cells. Nat. Immunol. *8*, 942–949. https://doi.org/10.1038/ni1496.

12. McGeachy, M.J., Chen, Y., Tato, C.M., Laurence, A., Joyce-Shaikh, B., Blumenschein, W.M., McClanahan, T.K., O'Shea, J.J., and Cua, D.J. (2009). The interleukin 23 receptor is essential for the terminal differentiation of interleukin 17-producing effector T helper cells in vivo. Nat. Immunol. *10*, 314–324. https://doi.org/10.1038/ni.1698.

13. Zúñiga, L.A., Jain, R., Haines, C., and Cua, D.J. (2013). Th17 cell development: from the cradle to the grave. Immunol. Rev. *252*, 78–88. https://doi.org/10.1111/imr.12036.

14. Scholzen, A., Mittag, D., Rogerson, S.J., Cooke, B.M., and Plebanski, M. (2009). Plasmodium falciparum-mediated induction of human CD25Foxp3 CD4 T cells is independent of direct TCR stimulation and requires IL-2, IL-10 and TGFbeta. PLoS Pathog. *5*, e1000543. https://doi.org/10.1371/journal.ppat.1000543.

15. Riley, E.M., Wahl, S., Perkins, D.J., and Schofield, L. (2006). Regulating immunity to malaria. Parasite Immunol. *28*, 35–49. https://doi.org/10.1111/j.1365-3024.2006.00775.x.

16. Finney, O.C., Riley, E.M., and Walther, M. (2010). Regulatory T cells in malaria–friend or foe? Trends Immunol. *31*, 63–70. https://doi.org/10.1016/j.it.2009.12.002.

17. Barnes, M.J., and Powrie, F. (2009). Regulatory T cells reinforce intestinal homeostasis. Immunity *31*, 401–411. https://doi.org/10.1016/j.immuni.2009.08.011.

18. Mills, K.H.G. (2004). Regulatory T cells: friend or foe in immunity to infection? Nat. Rev. Immunol. *4*, 841–855. https://doi.org/10.1038/nri1485.

19. Pflanz, S., Timans, J.C., Cheung, J., Rosales, R., Kanzler, H., Gilbert, J., Hibbert, L., Churakova, T., Travis, M., Vaisberg, E., et al. (2002). IL-27, a heterodimeric cytokine composed of EBI3 and p28 protein, induces proliferation of naive CD4+ T cells. Immunity *16*, 779–790. https://doi.org/10.1016/s1074-7613(02)00324-2.

20. Morita, Y., Masters, E.A., Schwarz, E.M., and Muthukrishnan, G. (2021). Interleukin-27 and Its Diverse Effects on Bacterial Infections. Front. Immunol. *12*, 678515. https://doi.org/10.3389/fimmu.2021.678515.

21. Mei, Y., Lv, Z., Xiong, L., Zhang, H., Yin, N., and Qi, H. (2021). The dual role of IL-27 in CD4+T cells. Mol. Immunol. *138*, 172–180. https://doi.org/10.1016/j.molimm.2021.08.001.

22. Jafarzadeh, A., Nemati, M., Chauhan, P., Patidar, A., Sarkar, A., Sharifi, I., and Saha, B. (2020). LeishmaniaInterleukin-27 Functional Duality Balances Infectivity and Pathogenesis. Front. Immunol. *11*, 1573. https://doi.org/10.3389/fimmu.2020.01573.

23. Fabbi, M., Carbotti, G., and Ferrini, S. (2017). Dual Roles of IL-27 in Cancer Biology and Immunotherapy. Mediators Inflamm. *2017*, 3958069. https://doi.org/10.1155/2017/3958069.

24. Morita, Y., Saito, M., Rangel-Moreno, J., Franchini, A.M., Owen, J.R., Martinez, J.C., Daiss, J.L., de Mesy Bentley, K.L., Kates, S.L., Schwarz, E.M., and Muthukrishnan, G. (2022). Systemic IL-27 administration prevents abscess formation and osteolysis via local neutrophil recruitment and activation. Bone Res. *10*, 56. https://doi.org/10.1038/s41413-022-00228-7.

25. Hölscher, C., Hölscher, A., Rückerl, D., Yoshimoto, T., Yoshida, H., Mak, T., Saris, C., and Ehlers, S. (2005). The IL-27 receptor chain WSX-1 differentially regulates antibacterial immunity and survival during experimental tuberculosis. J. Immunol. *174*, 3534–3544. https://doi.org/10.4049/jimmunol.174.6.3534.

26. Liu, Z., Liu, J.Q., Talebian, F., Wu, L.C., Li, S., and Bai, X.F. (2013). IL-27 enhances the survival of tumor antigen-specific CD8+ T cells and programs them into IL-10-producing, memory precursor-like effector cells. Eur. J. Immunol. *43*, 468–479. https://doi.org/10.1002/eji.201242930.

27. Gwyer Findlay, E., Villegas-Mendez, A., O'Regan, N., de Souza, J.B., Grady, L.M., Saris, C.J., Riley, E.M., Couper, K.N., and immunity. (2014). IL-27 receptor signaling regulates memory CD4+ T cell populations and suppresses rapid inflammatory responses during secondary malaria infection. Infection *82*, 10–20. https://doi.org/10.1128/iai.01091-13.

28. Budhu, S., Loike, J.D., Pandolfi, A., Han, S., Catalano, G., Constantinescu, A., Clynes, R., and Silverstein, S.C. (2010). CD8+ T cell concentration determines their efficiency in killing cognate antigen-expressing syngeneic mammalian cells in vitro and in mouse tissues. J. Exp. Med. *207*, 223–235. https://doi.org/10.1084/jem.20091279.

29. Pennock, N.D., Gapin, L., and Kedl, R.M. (2014). IL-27 is required for shaping the magnitude, affinity distribution, and memory of T cells responding to subunit immunization. Proc. Natl. Acad. Sci. USA *111*, 16472–16477. https://doi.org/10.1073/pnas.1407393111.

30. Klarquist, J., Chitrakar, A., Pennock, N.D., Kilgore, A.M., Blain, T., Zheng, C., Danhorn, T., Walton, K., Jiang, L., Sun, J., et al. (2018). Clonal expansion of vaccine-elicited T cells is independent of aerobic glycolysis. Sci. Immunol. *3*, eaas9822. https://doi.org/10.1126/sciimmunol.aas9822.

31. Intlekofer, A.M., Takemoto, N., Wherry, E.J., Longworth, S.A., Northrup, J.T., Palanivel, V.R., Mullen, A.C., Gasink, C.R., Kaech, S.M., Miller, J.D., et al. (2005). Effector and memory CD8+ T cell fate coupled by T-bet and eomesodermin. Nat. Immunol. *6*, 1236–1244. https://doi.org/10.1038/ni1268.

32. Marks-Konczalik, J., Dubois, S., Losi, J.M., Sabzevari, H., Yamada, N., Feigenbaum, L., Waldmann, T.A., and Tagaya, Y. (2000). IL-2-induced activation-induced cell death is inhibited in IL-15 transgenic mice. Proc. Natl. Acad. Sci. USA *97*, 11445–11450. https://doi.org/10.1073/pnas.200363097.

33. Kidder, B.L., Yang, J., and Palmer, S. (2008). Stat3 and c-Myc genome-wide promoter occupancy in embryonic stem cells. PLoS One *3*, e3932. https://doi.org/10.1371/journal.pone.0003932.

34. Morishima, N., Owaki, T., Asakawa, M., Kamiya, S., Mizuguchi, J., and Yoshimoto, T. (2005). Augmentation of effector CD8+ T cell generation with enhanced granzyme B expression by IL-27. J. Immunol. *175*, 1686–1693. https://doi.org/10.4049/jimmunol.175.3.1686.

35. Kilgore, A.M., Pennock, N.D., and Kedl, R.M. (2020). cDC1 IL-27p28 Production Predicts Vaccine-Elicited CD8 T Cell Memory and Protective Immunity. J. Immunol. *204*, 510–517. https://doi.org/10.4049/jimmunol.1901357.

36. Bradford, S.D., Witt, M.R., Povroznik, J.M., and Robinson, C.M. (2023). Interleukin-27 impairs BCG antigen clearance and T cell stimulatory potential by neonatal dendritic cells. Curr. Res. Microb. Sci. *4*, 100176. https://doi.org/10.1016/j.crmicr.2022.100176.

37. Christensen, D., Mortensen, R., Rosenkrands, I., Dietrich, J., and Andersen, P. (2017). Vaccine-induced Th17 cells are established as resident memory cells in the lung and promote local IgA responses. Mucosal Immunol. *10*, 260–270. https://doi.org/10.1038/mi.2016.28.

38. Zhang, Z., Clarke, T.B., and Weiser, J.N. (2009). Cellular effectors mediating Th17-dependent clearance of pneumococcal colonization in mice. J. Clin. Invest. *119*, 1899–1909. https://doi.org/10.1172/JCI36731.

39. Chen, Y., Shao, C., Fan, N.W., Nakao, T., Amouzegar, A., Chauhan, S.K., and Dana, R. (2021). The functions of IL-23 and IL-2 on driving autoimmune effector T-helper 17 cells into the memory pool in dry eye disease. Mucosal Immunol. *14*, 177–186. https://doi.org/10.1038/s41385-020-0289-3.

40. Kaminskiy, Y., and Melenhorst, J.J. (2022). STAT3 Role in T-Cell Memory Formation. Int. J. Mol. Sci. *23*, 2878. https://doi.org/10.3390/ijms23052878.

41. Geltink, R.I.K., Kyle, R.L., and Pearce, E.L. (2018). Unraveling the Complex Interplay Between T Cell Metabolism and Function. Annu. Rev. Immunol. *36*, 461–488. https://doi.org/10.1146/annurev-immunol-042617-053019.

42. Larocca, R.A., Provine, N.M., Aid, M., Iampietro, M.J., Borducchi, E.N., Badamchi-Zadeh, A., Abbink, P., Ng'ang'a, D., Bricault, C.A., Blass, E., et al. (2016). Adenovirus serotype 5 vaccine vectors trigger IL-27-dependent inhibitory CD4 T cell responses that impair CD8 T cell function. Sci. Immunol. *1*, eaaf7643. https://doi.org/10.1126/sciimmunol.aaf7643.

43. Jung, J.Y., and Robinson, C.M. (2014). IL-12 and IL-27 regulate the phagolysosomal pathway in mycobacteria-infected human macrophages. Cell Commun. Signal. *12*, 16. https://doi.org/10.1186/1478-811X-12-16.

44. Jung, J.Y., Roberts, L.L., and Robinson, C.M. (2015). The presence of interleukin-27 during monocyte-derived dendritic cell differentiation promotes improved antigen processing and stimulation of T cells. Immunology *144*, 649–660. https://doi.org/10.1111/imm.12417.

45. Seaver, K., Kourko, O., Gee, K., Greer, P.A., and Basta, S. (2022). IL-27 Improves Prophylactic Protection Provided by a Dead Tumor Cell Vaccine in a Mouse Melanoma Model. Front. Immunol. *13*, 884827. https://doi.org/10.3389/fimmu.2022.884827.

46. Wang, Y., Jiang, B., Guo, Y., Li, W., Tian, Y., Sonnenberg, G.F., Weiser, J.N., Ni, X., and Shen, H. (2017). Cross-protective mucosal immunity mediated by memory Th17 cells against Streptococcus pneumoniae lung infection. Mucosal Immunol. *10*, 250–259. https://doi.org/10.1038/mi.2016.41.

47. Batten, M., Li, J., Yi, S., Kljavin, N.M., Danilenko, D.M., Lucas, S., Lee, J., de Sauvage, F.J., and Ghilardi, N. (2006). Interleukin 27 limits autoimmune encephalomyelitis by suppressing the development of interleukin 17-producing T cells. Nat. Immunol. *7*, 929–936. https://doi.org/10.1038/ni1375.

48. Stumhofer, J.S., Laurence, A., Wilson, E.H., Huang, E., Tato, C.M., Johnson, L.M., Villarino, A.V., Huang, Q., Yoshimura, A., Sehy, D., et al. (2006). Interleukin 27 negatively regulates the development of interleukin 17-producing T helper cells during chronic inflammation of the central nervous system. Nat. Immunol. *7*, 937–945. https://doi.org/10.1038/ni1376.

49. Zhu, H., Lou, C., and Liu, P. (2015). Interleukin-27 ameliorates coxsackievirus-B3-induced viral myocarditis by inhibiting Th17 cells. Virol. J. *12*, 189. https://doi.org/10.1186/s12985-015-0418-x.

50. Visperas, A., Do, J.S., Bulek, K., Li, X., and Min, B. (2014). IL-27, targeting antigen-presenting cells, promotes Th17 differentiation and colitis in mice. Mucosal Immunol. *7*, 625–633. https://doi.org/10.1038/mi.2013.82.

51. Nefedova, Y., and Gabrilovich, D.I. (2007). Targeting of Jak/STAT pathway in antigen presenting cells in cancer. Curr. Cancer Drug Targets *7*, 71–77. https://doi.org/10.2174/156800907780006887.

52. Vallabhapurapu, S., and Karin, M. (2009). Regulation and function of NF-kappaB transcription factors in the immune system. Annu. Rev. Immunol. *27*, 693–733. https://doi.org/10.1146/annurev.immunol.021908.132641.

53. Kim, G., Shinnakasu, R., Saris, C.J.M., Cheroutre, H., and Kronenberg, M. (2013). A novel role for IL-27 in mediating the survival of activated mouse CD4 T lymphocytes. J. Immunol. *190*, 1510–1518. https://doi.org/10.4049/jimmunol.1201017.

54. Nish, S.A., Schenten, D., Wunderlich, F.T., Pope, S.D., Gao, Y., Hoshi, N., Yu, S., Yan, X., Lee, H.K., Pasman, L., et al. (2014). T cell-intrinsic role of IL-6 signaling in primary and memory responses. Elife *3*, e01949. https://doi.org/10.7554/eLife.01949.

55. Lunt, S.Y., and Vander Heiden, M.G. (2011). Aerobic glycolysis: meeting the metabolic requirements of cell proliferation. Annu. Rev. Cell Dev. Biol. *27*, 441–464. https://doi.org/10.1146/annurev-cellbio-092910-154237.

56. MacIver, N.J., Michalek, R.D., and Rathmell, J.C. (2013). Metabolic regulation of T lymphocytes. Annu. Rev. Immunol. *31*, 259–283. https://doi.org/10.1146/annurev-immunol-032712-095956.

57. Montes de Oca, M., de Labastida Rivera, F., Winterford, C., Frame, T.C.M., Ng, S.S., Amante, F.H., Edwards, C.L., Bukali, L., Wang, Y., Uzonna, J.E., et al. (2020). IL-27 signalling regulates glycolysis in Th1 cells to limit immunopathology during infection. PLoS Pathog. *16*, e1008994. https://doi.org/10.1371/journal.ppat.1008994.

STAR★METHODS

KEY RESOURCES TABLE

REAGENT or RESOURCE	SOURCE	IDENTIFIER
Antibodies		
PE anti-mouse FOXP3 Antibody	Biolegend	Cat # 126404; RRID: AB_1089117
FITC anti-mouse CD25 Antibody	Biolegend	Cat # 102006; RRID: AB_312855
Purified anti-mouse CD16/32 Antibody	Biolegend	Cat # 101302; RRID: AB_312801
Brilliant Violet 650™ anti-mouse CD4 Antibody	Biolegend	Cat# 116027; RRID: AB_2800581
PE-Cyanine 7 anti-mouse IFN-γ Antibody	Biolegend	Cat# 505826; RRID: AB_2295770
Brilliant Violet 421™ anti-mouse IL-5 Antibody	Biolegend	Cat# 504311; RRID: AB_2563161
Brilliant Violet 421™ anti-mouse IL-17A Antibody	Biolegend	Cat# 506926; RRID: AB_2632611
APC anti-mouse CD44 Antibody	Biolegend	Cat# 103012; RRID: AB_312963
Alexa Fluor® 700 anti-mouse CD62L Antibody	Biolegend	Cat# 104426; RRID: AB_493719
PerCP/Cyanine5.5 anti-mouse CD127 Antibody	Biolegend	Cat# 135021; RRID: AB_1937274
Alexa Fluor® 488 anti-mouse p-STAT3 Antibody (Tyr 705)	Biolegend	Cat# 651005; RRID: AB_2572083
Recombinant Anti - beta Actin Rabbit mAb	servicebio, China	Cat # GB15003
Stat3 (124H6) Mouse mAb	Cell Signaling Technology	Cat # 9139; RRID: AB_331757
Phospho-Stat3 (Tyr705) (D3A7) XP® Rabbit mAb	Cell Signaling Technology	Cat # 9145; RRID: AB_2491009
Phospho-NF-κB p65 (Ser536) (93H1) Rabbit mAb	Cell Signaling Technology	Cat # 3033; RRID: AB_331284
Goat anti-rabbit IgG-HRP Antibody	Cell Signaling Technology	Cat # 7074; RRID: AB_2099233
Goat anti-mouse IgG-HRP Antibody	Cell Signaling Technology	Cat # 7056; RRID: AB_330921
Anti -CD68 Rabbit pAb	servicebio, China	Cat # GB113109; RRID: AB_2935658
Anti -Ly6G Rabbit pAb	servicebio, China	Cat # GB11229; RRID: AB_2814689
Goat anti-Rabbit-HRP	servicebio, China	Cat # GB23303; RRID: AB_2811189
Bacterial and virus strains		
Streptococcus pneumoniae	NCTC	7466
Streptococcus pneumoniae	CMCC(B)	31693
SPY1	This paper	N/A
Chemicals, peptides, and recombinant proteins		
Cholera Toxin	Sigma	Cat #C8052-2MG
Murine IL-4	PeproTech	Cat# 214-14-20ug
Murine GM-CSF	PeproTech	Cat# 315-03-20ug
Recombinant Mouse IL-27	Biolegend	Cat# 577406
2-Deoxy-D-glucose	MedChemExpress	Cat# HY-13966
Fixative Solution (4% formaldehyde, methanol-free)	Biosharp	Cat# BL539A
BASIC RPMI 1640 Medium	Invitrogen/Gibco	Cat #C11875500BT
Red Blood Cell Lysis Buffer	Biosharp Life science	Cat # BL503A
RNAiso Plus reagent	TaKaRa	Cat # 9108
Critical commercial assays		
PrimeScript™RT Reagent kit (Perfect Real Time)	TaKaRa	Cat # RR037A
SYBR Green Master Mix	TsingkeBiotechnology Co., Ltd.	Cat # TSE202
Mouse IL-23 DuoSet ELISA	R&D Systems	Cat# DY1887-05
Mouse IL-27p28 DuoSet ELISA	R&D Systems	Cat# DY1834

(*Continued on next page*)

Continued

REAGENT or RESOURCE	SOURCE	IDENTIFIER
ELISA MAX™ Deluxe Set Mouse IFN-γ	Biolegend	Cat # 430804
Mouse TGF-beta 1 DuoSet ELISA	R&D Systems	Cat # DY1679-05
ELISA MAX™ Deluxe Set Mouse IL-17A	Biolegend	Cat # 432504
ELISA MAX™ Deluxe Set Mouse IL-5	Biolegend	Cat # 431204
ELISA MAX™ Deluxe Set Mouse IL-6	Biolegend	Cat # 431304
ELISA MAX™ Deluxe Set Mouse IL-1β	Biolegend	Cat # 432604
Deposited data		
Raw and analyzed data	This paper	Figshare: https://doi.org/10.6084/m9.figshare.23816610
Experimental models: Organisms/strains		
Mouse: B6N.129P2-IL-27rαtm1Mak/J	The Jackson Laboratory	RRID: IMSR_JAX:018078
Mouse:C57BL/6J	Chongqing Medical University	RRID: IMSR_JAX:000664
Oligonucleotides		
Primers for qPCR, see Table S1	This paper	N/A
Software and algorithms		
GraphPad Prism 7.0	GraphPad Software	https://www.graphpad-prism.cn
FlowJoTM v10.6.2	FlowJo Software	https://www.flowjo.com/
ImageJ	ImageJ Software	https://imagej.nih.gov/ij/

RESOURCE AVAILABILITY

Lead contact

Further information and requests for resources and reagents should be directed to and will be fulfilled by the lead contact, Wenchun Xu (xuwen@cqmu.edu.cn).

Materials availability

This study did not generate new unique reagents.

Data and code availability

Data have been deposited at Figshare and are publicly available as of the date of publication. DOIs are listed in the key resources table.This paper does not report original code. Any additional information required to reanalyze the data reported in this paper is available from the lead contact upon request.

EXPERIMENTAL MODEL AND STUDY PARTICIPANT DETAILS

Animal

IL-27Rα$^{-/-}$ mice (The Jackson Laboratory, Bar Harbor, ME, USA) and C57BL/6J mice (Chongqing Medical University, Chongqing, China) were used in this study. All experimental animals were healthy 6-8weeks-old female mice weighing 18 to 20g. C57BL/6J and IL-27Rα$^{-/-}$ mice were randomly divided into immunized and control groups. In the SPY1 vaccine immunization model, mice were anesthetized with pentobarbital. SPY1 strains (1 × 10^8 CFU) combined with cholera toxin adjuvants (1μg) or adjuvant alone (CT + PBS) was slowly instilled into the nostrils of mice. A total of 4 doses of immunization were administered with a one-week interval. Specimens were collected for analysis one week after the last immunization. In the pneumococcal challenge model, one week following the last immunization, C57BL/6J mice and IL-27Rα$^{-/-}$ mice were challenged intranasally with *S. pneumoniae* strain 19F (1.5 × 10^8 CFU). Specimens were collected for analysis three days after challenge. In the survival experiment, one week following the last immunization, mice were challenged intranasally with *S. pneumoniae* strain D39 (5 × 10^7 CFU). The status of mice was observed 21 days after challenge. In the 2-DG treatment experiments, in the process of SPY1 vaccine immunization and 19F challenge, PBS or 2-DG (MedChemExpress, Monmouth Junction, NJ, USA) was injected intraperitoneally every day, and the concentration of 2-DG was 1 g/kg. For the establishment of

memory models, C57BL/6J mice and IL-27Rα$^{-/-}$ mice were immunized with SPY1 vaccine, and lung tissues were collected two weeks after the last immunization for analysis.

Mice were housed under specific pathogen-free conditions. All animal experiments were performed in accordance with the specifications and requirements of the Laboratory Animal Center of Chongqing Medical University.

Primary cell

Bone marrow cells were washed out from the femurs and tibia of healthy female mice following sacrifice with pentobarbital. Red blood cells were removed and the remaining cells were suspended in RPMI 1640 containing 10% heat-inactivated fetal bovine serum (Ausbian, Sydney, Australia), 100U penicillin/100 μg streptomycin, 20 ng/mL rGM-CSF and 10 ng/mL rIL-4 (PeproTech, Cranbury, NJ, USA). The cells were incubated in 5% CO_2 at 37°C. The medium was replaced on days 3 and 5 and the suspended and loosely attached cells (immature DC) were collected on days 6 or 7. Cells were plated in six-well plates at 2×10^6 cells per well and treated with 5×10^7CFU of ethanol-inactivated SPY1 for 24h. Cell supernatants and cells were collected for analysis.

Strain

S. pneumoniae strains used for these experiments included D39 (Serotype 2, NCTC 7466 National Collection of Type Cultures, London, UK) and CMCC(B) 31693 (Serotype 19F, Center for Medical Culture Collections, Beijing, China). Strain SPY1 was generated in our laboratory by repeated serial passage of strain D39. All bacterial strains were cultured in casein medium containing yeast extract (C + Y medium) or on Columbia sheep blood agar plates at 37°C in a 5% CO_2 atmosphere. SPY1 was used as the immunogen and cultured in C + Y medium at 37°C under 5% CO_2 to 1×10^8 CFU/mL equivalent to an OD_{620} of 0.5. The bacteria were collected by centrifugation and washed twice with sterile phosphate buffered saline (PBS) and then suspended in PBS. The final vaccine mixture contained 1×10^8 CFU SPY1 and 1μg of adjuvant cholera toxin (CT; Sigma, St. Louis, MO, USA).

METHOD DETAILS

Flow cytometry analysis

Mouse lungs were removed and single cell suspensions were prepared for flow analysis. Tregs ($CD4^+$-$CD25^+Foxp3^+$) were detected by incubation of lung cells with anti-CD16/CD32 and then stained with anti-mouse BV605-CD4 and FITC-CD25. Cells were lysed and fixed in Fix/Perm buffer and blocked again with anti-CD16/CD32 antibody and then incubated with anti-mouse PE-Foxp3. Th1 ($CD4^+$IFN-γ^+), Th2 ($CD4^+$IL-5^+) and Th17 ($CD4^+$IL-$17A^+$) cells were detected by incubating lung tissue cells with 2 mL RPMI 1640 containing cell stimulation mix (Thermo Fisher Scientific, Waltham, MA, USA) at 37°C-5% CO_2 for 4–6 h. Cells were subsequently collected by centrifugation and blocked with anti-CD16/CD32 antibody and then stained with anti-mouse BV605-CD4. Then cells were lysed and fixed in Fix/Perm buffer and blocked again with anti-CD16/CD32 antibody. The cells were then incubated with anti-mouse PE-Cy7-IFN-γ and BV421-IL-5 and BV421-IL-17A. Memory $CD4^+$T cells were detected in lung tissue cells by incubation with anti-CD16/CD32 followed by Biolegend antibodies anti-mouse BV605-CD4, APC-CD44, AF-700-CD62L and Percp-Cy5.5-CD127. Phosphorylated proteins were analyzed by suspending cells in 1.5% formaldehyde followed by fixed at 37°C for 15 min and cell lysis by the addition of methanol precooled followed by 15 min on ice. This lysate was used for detection of intracellular phosphorylated proteins with the antibody AF-488-p-STAT3 for 1 h prior to flow cytometric analysis.

RT-PCR analysis

Total RNA was extracted from cells using RNAiso Plus (Takara Bio, Dalian, China) following the manufacturers protocol. Total RNA was reverse transcribed into cDNA according to the instructions of the reverse transcription kit (Takara Bio). Target gene expression levels were quantified using a Bio-Rad CFX96 Real-Time system using SYBR Premix Ex Taq (TsingkeBiotechnology Co., Ltd.). The primer pairs used in the study are listed in Table S1. PCR primers were synthesized by Sangon (Shanghai, China)

Cytokine analysis

Cytokines were detected from lung and spleen homogenates. Mice BMDC were induced (see above) and exposed to *S. pneumoniae* strain SPY1 previously inactivated by suspension 70% ethanol for 24 h. IL-17A,

IL-5, IL-1β, IFN-γ and IL-6 levels were detected using a commercial kit (ELISA MAX Deluxe, Biolegend). IL-27 p28, TGF-β and IL-23 were measured using the ELISA Duoset kit (R&D Systems, Minneapolis, MN, USA).

Antibody titer analysis

One week following the last intranasal immunization (see above), blood samples were collected from tail veins and serum was isolated to establish baseline antibody levels. And the mice were intraperitoneally injected with 40 μL carbachol and saliva samples were collected. The assays were conducted in 96-well microplate coated with SPY1 OD_{620} = 0.1 overnight and then blocked in 1% PBST containing 2% BSA for 2 h. Gradient dilutions of mouse serum or saliva were added and HRP-labeled goat anti-mouse IgG and IgA (Santa Cruz Biotechnology, Dallas, Texas, USA) were then added and TBM substrate (Biolegend) were used for color development according to the manufacturer's guidelines. The maximum dilution corresponding to A450 $\geq$ 2.1 times the mean value of the negative control wells was used as the specific antibody titer.

Western Blot analysis

BMDC whole cell lysates were generated using RIPA buffer containing PMSF and proteins were separated in 10% SDS-PAGE gels and electro-transferred to PVDF membranes and used for Western blot analysis. Primary antibodies used for Western blotting were anti-mouse β-actin (servicebio, Wuhan, China), anti-mouse STAT3(Cell Signaling Technology, Danvers, MA, USA), anti-mouse phospho-STAT3(Cell Signaling Technology) and anti-mouse phospho-NF-κB p65(Cell Signaling Technology). Protein bands were visualized utilizing HRP-conjugated anti-mouse secondary antibodies coupled with ECL detection.

Immunohistochemistry and HE staining

Lung tissues were obtained from mice 3 days after 19F challenge, perfused with paraformaldehyde and fixed overnight by immersion in paraformaldehyde then embedded in paraffin and cut into 5 mm sections and mounted on slides. The slides were stained with hematoxylin and eosin (H&E) and viewed using light microscopy. Tissue sections were also stained with polyclonal goat anti-mouse CD68 and Ly6G (servicebio) and detected using a streptavidin biotin immuno-peroxidase system. The inflammatory degree was measured double blind using a numerical scoring system: 0 = no inflammation; 1 = occasional cuffing with inflammatory cells; 2 = most bronchi and vessels were surrounded by a thin layer (1–2 cells); 3 = a moderate layer (3–5 cells); 4 = a thick layer (>5 cells). The total inflammation score was calculated by the addition of both peribronchial and perivascular inflammation scores (10 per mouse).

QUANTIFICATION AND STATISTICAL ANALYSIS

All of the statistical details for each experiment can be found in the figure legends. All data in this study are presented as mean ± SEM and analyzed using one-way ANOVA or unpaired Student's *t* test. Survival was compared using the Log rank test. Graphpad7.0 software was used for mapping and statistical analysis, and $p < 0.05$ was considered statistically significant.